

Thermoelectric transport across a tunnel contact between two charge Kondo circuits

T. K. T. Nguyen,^{1,*} H. Q. Nguyen,¹ and M. N. Kiselev²

¹*Institute of Physics, Vietnam Academy of Science and Technology, 10 Dao Tan, 118000 Hanoi, Vietnam*

²*The Abdus Salam International Centre for Theoretical Physics, Strada Costiera 11, I-34151, Trieste, Italy*
(Dated: June 22, 2023)

Following a theoretical proposal on multi-impurity charge Kondo circuits [T. K. T. Nguyen and M. N. Kiselev, Phys. Rev. B **97**, 085403 (2018)] and the experimental breakthrough in fabrication of the two-site Kondo simulator [W. Pouse *et al*, Nat. Phys. (2023)] we investigate a thermoelectric transport through a double-dot charge Kondo quantum nano-device in the strong coupling operational regime. We focus on the fingerprints of the non-Fermi liquid and its manifestation in the charge and heat quantum transport. We construct a full-fledged quantitative theory describing crossovers between different regimes of the multi-channel charge Kondo quantum circuits and discuss possible experimental realizations of the theory.

I. INTRODUCTION

Thermoelectric materials have been investigated in recent years thanks to their ability to generate electricity from waste heat or being used as solid-state Peltier coolers [1]. The mechanism of converting of heat into voltage known as the Seebeck effect [2] is associated with the emergence of the electrostatic potential across the *hot* and *cold* ends of the *thermocouple* [3, 4] while no electric current flows through the system. The Peltier effect is manifested by the creation of the temperature difference between the junctions when the electric current flows through the *thermocouple*.

After theoretical predictions have been suggested that the thermoelectric efficiency could be greatly enhanced through nano-structural engineering in the mid-1990s, many complex nano-structured materials were studied in both theory and experiment [5–8]. Nano-electric circuits based on one or a few quantum dots (QDs), which are highly controllable and fine-tunable, can provide important information about the effects of strong electron-electron interactions, interference effects and resonance scattering on the quantum charge, spin and heat transport.

One of the fundamental motivations of the thermoelectric studies is to enhance thermoelectric power (absolute value of the Seebeck coefficient, TP). It is a challenge for both experimental fabrication of devices and theoretical suggestions for efficient mechanisms of heat transfer. In fact, the theoretical investigations showed that the TP of a single electron transistor (SET) was greatly enhanced in comparison with those of bulk materials [9, 10]. Furthermore, the charge Kondo effect [11–13, 15, 16] dealing with the degeneracy of the charge states of the QD (which is similar to the conventional Kondo effect [17–21] but does not require the system to have magnetic degree of freedom) can be a tool for intensification of the TP of a SET [14, 22]. The building block of a charge Kondo circuit (CKC) is a large metallic QD strongly coupled to one (or several) lead(s) through

an (or several) almost transparent single-mode quantum point contact(s) [QPC(s)]. In the *orthodox* charge Kondo theory [11–13], the electron location (namely, in or out of QD) is treated as an iso-spin variable, while two spin projections of electrons are associated with two (degenerate, in the absence of external magnetic field) conduction channels in the conventional Kondo problem. External magnetic field lifts out the channel degeneracy resulting in a crossover from two channel Kondo (2CK) regime at the vanishing magnetic field to the single channel Kondo (1CK) regime at the strong external field [23]. As a result, the behavior of the system continuously changes from non-Fermi liquid (NFL) to the Fermi liquid (FL) states respectively. The interplay between NFL-2CK and FL-1CK regimes in thermoelectric transport through the SET has been investigated [16, 23–29]. The charge transport in 1CK and 2CK regimes were studied extensively numerically in Refs.[30–33]. The effects of the electron-electron interactions in the charge Kondo simulators have been considered recently [26, 28, 34, 35].

Recently, CKCs operated in the integer quantum Hall (IQH) regime have been implemented in breakthrough experiments [36, 37]. With the advantage that the number of Kondo channels is determined by the number of QPCs attached to the metallic QD, these experiments have opened an access to investigation of the multi-channel Kondo (MCK) problem experimentally. The dominant characteristic of a specific MCK setup is a NFL picture [38–40] which is associated with Z_M symmetry. For instance, the NFL-2CK [41–43] is explained by Majorana fermions [44, 45], the NFL-3CK physics is related to Z_3 parafermions [46–51]. Therefore, switching between Z_{2k+1} and Z_{2k} low temperature fixed points by controlling the reflection amplitudes of the QPCs, can provide a route to investigate the crossovers between states with different parafermion fractionalized zero modes [52].

As a CKC is considered as an artificial quantum simulator for the technology of quantum computer, scaling up the CKCs to clusters or lattices is challenging and it is important to understand the nature of the coupling between neighboring QDs. For this motivation, the

* nkthanh@iop.vast.vn

experiment [53] has implemented a two-island charge Kondo device in which two QDs are coupled together and each one is also strongly coupled to an electrode through a QPC. The authors investigated the quantum phase transition at the triple point where the charge configurations are degenerate. Being more than the two-impurity Kondo (2IK) model, the two-site charge Kondo circuit is relevant to the Kondo lattice systems. Furthermore, the deeper theoretical investigation of the strong central coupling of this setup [54, 55] in the Toulouse limit showed that a Z_3 parafermion emerging at the critical point, was already present in the experimental device of Ref. [53].

In this work, we revisit the model proposed in Ref. [25] which contains a tunnel contact between two CKCs where each one is set up in either FL or NFL state (see Fig. 1) with a two-fold goal. First, we examine the behavior of TP in order to find a mechanism to enhance it. Secondly, we show the existence of Majorana fermions in this double charge Kondo circuit (DCKC). The non-perturbative solution is obtained which allows to monitor and control all FL-NFL crossovers. The new energy scale associated with the inverse lifetime of the emergent Majorana fermions controls four different regimes of thermoelectric transport based on the window of parameters. Moreover, the non-perturbative results reported in this paper complete a full-fledged theory of the non-Fermi liquid to Fermi liquid crossover in the DCKC.

The paper is organized as follows. We describe the proposed experimental setup and the theoretical model in Sec. II. General equations for the thermoelectric coefficients are presented and the nonperturbative solution is discussed in Sec. III. The Sec. IV represents the correlation function in different cases. The main results are discussed in Sec. V. We conclude our work in Sec. VI.

II. PROPOSED EXPERIMENTAL SETUP AND THEORETICAL MODEL

We consider a DCKC device (see Fig. 1) formed by two CKCs describing a very recent experiment [53]. The building block for each CKC is a QD-QPC structure implemented in experiment [36]. The QD is a large metallic island (the dark-red and blue cross-hatched areas surrounded by the black lines) electronically connected to a two-dimensional electron gas (2DEG, the orange and grey continuous areas). The 2DEG is connected to two large electrodes through two QPCs. Applying a strong magnetic field perpendicular to the 2DEG plane can control the 2DEG in the IQH regime at the filling factor $\nu = 1$. The QPCs are fine-tuned (by field effects in the split gates illustrated by the blue boxes) to the high transparency regime corresponding to weak backscattering of the chiral edge mode (red solid lines with arrows). We investigate the regime of equal reflection amplitudes at two QPCs in each CKC: $|r_{11}| = |r_{12}| = |r_1|$ and $|r_{21}| = |r_{22}| = |r_2|$. Therefore, each CKC is a 2CK

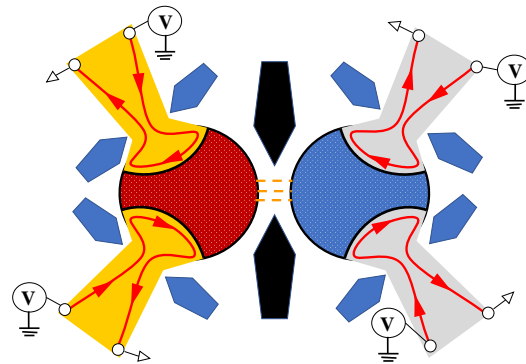


FIG. 1. Schematic of a weak link between two charge Kondo circuits (CKC). Each circuit consists of a large metallic island (QD), which is embedded into two-dimensional electron gas (2DEG) and connects to two large electrodes through the single-mode quantum point contacts (QPCs). The 2DEG (plain area) is in the integer quantum Hall regime $\nu = 1$. The red line with arrows denotes the chiral edge mode which backscatters at the center of the narrow constriction. The QPCs are fine tuned by field effects in split gates (blue boxes) to different regimes. We name the QPCs in the left CKC as QPC₁₁, QPC₁₂ and the QPCs in the right CKC as QPC₂₁, QPC₂₂. The right CKC (grey color) is at the reference temperature T while the left circuit (orange color) is at higher temperature $T + \Delta T$.

setup. Indeed, the CKC can be tuned into a 1CK model by simply deactivating one of the two QPCs in it. These two CKCs are connected together by a weak tunneling (barrier, weak link) between two QDs. In order to study the thermoelectric transport through the DCKC system, the left CKC is set up at higher temperature $T + \Delta T$ in comparison with the right circuit, which is at temperature T . The temperature drops at the central weak link.

The spinless Hamiltonian describing the two CKCs coupled weakly at the center in which each QD is coupled strongly to the lead through two QPCs (Fig. 1) has the form $H = H_L + H_T + H_R$, where

$$H_T = (td_1^\dagger d_2 + \text{h.c.}). \quad (1)$$

describes the tunneling between two dots, d_j stands for the electrons in the dot j , $j = 1, 2$. The Hamiltonian $H_{L/R}$ describing each (QD-QPC) structure has the form $H_{L/R} = H_{0L/R} + H_{CL/R} + H_{sL/R}$. The Hamiltonian $H_{0,j}$ ($j = L, R$) describing the propagation of the edge states is given by

$$H_{0,j} = -iv_F \sum_{\alpha=1,2} \int_{-\infty}^{\infty} dx \left[\psi_{R,j,\alpha}^\dagger(x) \partial_x \psi_{R,j,\alpha}(x) - \psi_{L,j,\alpha}^\dagger(x) \partial_x \psi_{L,j,\alpha}(x) \right], \quad (2)$$

where $\psi_{L/R,\alpha,j}$ represents the incoming/outgoing chiral fermions at the QPC α of the CKC j , and v_F is the Fermi velocity. For simplicity we assume that the Fermi velocity is the same for all QPCs. Note that the operator d_j can be expressed through the fermionic operators

$\psi_{j,\alpha}$ as $d_j = \sum_{\alpha=1,2} \psi_{j,\alpha}(-\infty)$. The Hamiltonian $H_{C,j}$ characterizes the Coulomb interaction in the dot [14, 56]

$$H_{C,j} = E_{C,j} \int_0^\infty dx \left[n_j - \sum_{\alpha=1,2} \psi_{j,\alpha}^\dagger(x) \psi_{j,\alpha}(x) - N_j \right]^2, \quad (3)$$

where $E_{C,j}$ is the charging energy of the QD j . The number of electrons entering the dot (taking values 0, 1 in units of e) through the weak link and the QPCs is demonstrated by the operator n_j and the second term in the parentheses (with $\psi_{j,\alpha} = \psi_{L,j,\alpha} + \psi_{R,j,\alpha}$) respectively. N_j is the normalized gate voltage, controlled by plunger gates (not shown in Fig. 1). The Hamiltonian $H_{s,j}$ describing the backward scattering at the QPCs, with the reflection amplitude $r_{j,\alpha}$, writes

$$H_{s,j} = -\frac{D}{\pi} \sum_{\alpha=1,2} |r_{j,\alpha}| \left[\psi_{R,j,\alpha}^\dagger(0) \psi_{L,j,\alpha}(0) + h.c. \right], \quad (4)$$

D is a bandwidth.

The appropriate technique to describe the interacting electrons in the QD and QPCs is the bosonized representation [44, 57]. The detailed bosonization of the Hamiltonian H can be read in Refs. [14, 25]. One should notice that the fermionic fields are related to the bosonic field at the QPC α of the CKC j as $\psi_{L/R,j,\alpha}(x) \sim e^{-i\phi_{j,\alpha}(x)}$. The actions in the bosonic language are presented in the Section IV.

III. GENERAL FORMULAS FOR CURRENT, ELECTRIC CONDUCTANCE AND THERMOELECTRIC COEFFICIENT

In order to study the thermoelectric effects in the DCKC with a small temperature drop $\Delta T \ll T$ at the weak link between two QDs, we consider the tunnel charge current across the tunnel contact in the tunneling amplitude $|t|$ as

$$I = -2\pi e |t|^2 \int_{-\infty}^{\infty} d\epsilon \nu_1(\epsilon) \nu_2(\epsilon) [f_1(\epsilon) - f_2(\epsilon)]. \quad (5)$$

Here we denote the Fermi distribution functions as $f_1(\epsilon) = f(\epsilon, T + \Delta T)$, $f_2(\epsilon) = f(\epsilon + e\Delta V, T)$, with ΔV is an applied thermo-voltage to implement a zero-current condition for the electric current between the source and drain, and we define the densities of states $\nu_j(\epsilon) = -(1/\pi) \cosh\left(\frac{\epsilon}{2T}\right) \int_{-\infty}^{\infty} \mathcal{G}_j((1/2T) + it) e^{i\epsilon t} dt$ with $\mathcal{G}_j(\tau) = -\langle T_\tau d_j(\tau) d_j^\dagger(0) \rangle$ are exact Green's Functions (GF) in the terminals $j = 1, 2$. The thermoelectric coefficients in the linear response regime are computed as follows. The electric conductance casts a form

$$G = \left. \frac{\partial I}{\partial \Delta V} \right|_{\Delta T=0} = \frac{e^2 |t|^2}{2\pi T} \int_{-\infty}^{\infty} d\epsilon \int_{-\infty}^{\infty} dt_1 \times \mathcal{G}_1 \left(\frac{1}{2T} + it_1 \right) e^{i\epsilon t_1} \int_{-\infty}^{\infty} dt_2 \mathcal{G}_2 \left(\frac{1}{2T} + it_2 \right) e^{i\epsilon t_2}, \quad (6)$$

and the thermoelectric coefficient is given by

$$G_T = \left. \frac{\partial I}{\partial \Delta T} \right|_{\Delta V=0} = -\frac{e|t|^2}{2\pi T^2} \int_{-\infty}^{\infty} d\epsilon \int_{-\infty}^{\infty} dt_1 \mathcal{G}_1 \left(\frac{1}{2T} + it_1 \right) e^{i\epsilon t_1} \int_{-\infty}^{\infty} dt_2 \mathcal{G}_2 \left(\frac{1}{2T} + it_2 \right) e^{i\epsilon t_2}. \quad (7)$$

The thermopower (or the Seebeck coefficient) in the linear regime is defined at $I = 0$ as

$$S = - \left. \frac{\Delta V}{\Delta T} \right|_{I=0} = \frac{G_T}{G}. \quad (8)$$

Following Matveev and Andreev [14] we define $d_j(\tau) = \psi_{j,\alpha}^{(0)}(\tau) F_j(\tau)$, where $\psi_{j,\alpha}^{(0)}(\tau) = \psi_{\alpha,j}^{(0)}(-\infty, \tau)$, the operator F_j obeys the commutation relation $[F_j, n_j] = F_j$ and takes into account effects of interaction and reflection given by Eqs. (3,4). Since the operators $\psi_{j,\alpha}^{(0)}$ and F_j are decoupled, the GFs at imaginary times are factorized as $\mathcal{G}_j(\tau_j) = -(\nu_{0j} \pi T / \sin[\pi T \tau_j]) K_j(\tau_j)$, where ν_{0j} is the density of states in the dot j without interaction and $K_j(\tau) = \langle T_\tau F_j(\tau) F_j^\dagger(0) \rangle$ accounts for interaction effects. As a result, the electric conductance and the thermoelectric coefficient are given by:

$$G = \frac{\pi}{2} G_C T \int_{-\infty}^{\infty} \frac{dt}{\cosh^2(\pi T t)} K_1 \left(\frac{1}{2T} + it \right) K_2 \left(\frac{1}{2T} - it \right), \quad (9)$$

$$G_T = -\frac{i\pi G_C}{4e} \int_{-\infty}^{\infty} \frac{dt}{\cosh^2(\pi T t)} \times \left[\left(\partial_t K_1 \left(\frac{1}{2T} + it \right) \right) K_2 \left(\frac{1}{2T} - it \right) - K_1 \left(\frac{1}{2T} + it \right) \left(\partial_t K_2 \left(\frac{1}{2T} - it \right) \right) \right], \quad (10)$$

where $G_C = 2\pi e^2 \nu_{01} \nu_{02} |t|^2$ is a conductance of the central (tunnel) area. The computation of thermoelectric coefficients in Eqs. (9-10) [58] requires the explicit form of the correlation functions $K_{1,2}(\frac{1}{2T} \pm it)$.

IV. CORRELATION FUNCTION $K_j(\tau)$:

The time-ordered correlation function $K_j(\tau)$ is defined through the operator F_j . The process where the number of electron entering the QD _{j} through the weak link is increased from 0 to 1 at time $t = 0$ and decreased back to 0 at time $t = \tau$ is demonstrated by $F_j(\tau) F_j^\dagger(0)$. Therefore, the operator n_j is replaced by $n_{j\tau}(t) = \theta(t) \theta(\tau - t)$ with $\theta(t)$ is the unit step function, and the correlation function $K_j(\tau)$ is computed through the functional integration over the bosonic fields $K_j(\tau) = Z_j(\tau)/Z_j(0)$.

A. The 1CK case: Perturbative solution:

In the case one CKC is settled down in the FL-1CK state by decoupling one of the two QPCs, the functional integral writes

$$Z_j(\tau) = \int \mathcal{D}\phi_j \exp[-\mathcal{S}_{0,j} - \mathcal{S}_{C,j}(\tau) - \mathcal{S}_{s,j}], \quad (11)$$

where $\mathcal{S}_{0,j}$, $\mathcal{S}_{C,j}$, and $\mathcal{S}_{s,j}$ are Euclidean actions describing the free (non-interacting) one-dimensional Fermi gas, Coulomb blockade in the QD and the backscattering at the QPC of the CKC j , respectively. They are written as

$$\mathcal{S}_{0,j} = \frac{v_F}{2\pi} \int_0^\beta dt \int dx \left[\frac{(\partial_t \phi_j)^2}{v_F^2} + (\partial_x \phi_j)^2 \right], \quad (12)$$

$$\mathcal{S}_{C,j} = E_{C,j} \int_0^\beta dt \left[n_{j\tau}(t) + \frac{1}{\pi} \phi_j(0, t) - N_j \right]^2, \quad (13)$$

$$\mathcal{S}_{s,j} = -\frac{2D}{\pi} |r_j| \int_0^\beta dt \cos[2\phi_j(0, t)]. \quad (14)$$

with $\beta = 1/T$. One should notice that the bosonic field describing the electrons moving through the constriction is blocked by the Coulomb interaction in the QD. Therefore, $Z_j(\tau)$ can be computed perturbatively over $|r_j|$ for the small backscattering at the QPC ($|r_j| \ll 1$), and the correlation function $K_j(\tau)$ then is

$$K_j(\tau) = \left(\frac{\pi^2 T}{\gamma E_{C,j}} \right)^2 \frac{1}{\sin^2(\pi T \tau)} [1 - 2\gamma \xi |r_j| \cos(2\pi N_j) + 4\pi^2 \xi \gamma |r_j| \frac{T}{E_{C,j}} \sin(2\pi N_j) \cot(\pi T \tau)], \quad (15)$$

with $\gamma = e^C$, $C \approx 0.577$ is Euler's constant, $\xi = 1.59$ is a numerical constant [14].

B. The symmetric 2CK case: Nonperturbative solution:

For convenient calculation later, one can define the variables $\phi_{j,\rho/\sigma} = \phi_{j,1} \pm \phi_{j,2}$ so-called charge/spin fields. The functional integral in this case is written as:

$$Z_j(\tau) = \prod_{\lambda=\rho,\sigma} \int \mathcal{D}\phi_{j,\lambda} \exp[-\mathcal{S}_{0,j} - \mathcal{S}_{C,j}(\tau) - \mathcal{S}_{s,j}], \quad (16)$$

where $\mathcal{S}_{0,j}$, $\mathcal{S}_{C,j}$, and $\mathcal{S}_{s,j}$ are Euclidean actions describing the free Fermi liquid, Coulomb blockade in the QD and the backscattering at the QPCs of the CKC j , respectively. The action $\mathcal{S}_{0,j}$ is presented as a sum of two independent actions

$$\mathcal{S}_{0,j} = \sum_{\lambda=\rho,\sigma} \frac{v_F}{2\pi} \int_0^\beta dt \int dx \left[\frac{(\partial_t \phi_{j,\lambda})^2}{v_F^2} + (\partial_x \phi_{j,\lambda})^2 \right]. \quad (17)$$

The Coulomb blockade action $\mathcal{S}_{C,j}$ in bosonic representation reads

$$\mathcal{S}_{C,j} = E_{C,j} \int_0^\beta dt \left[n_{j\tau}(t) + \frac{\sqrt{2}}{\pi} \phi_{j,\rho}(0, t) - N_j \right]^2. \quad (18)$$

The contribution $\mathcal{S}_{s,j}$ in the action of each CKC characterizes the weak backscattering at the QPCs is

$$\mathcal{S}_{s,j} = -\frac{2D}{\pi} |r_j| \int_0^\beta dt \cos \left[\sqrt{2} \phi_{j,\rho}(0, t) \right] \cos \left[\sqrt{2} \phi_{j,\sigma}(0, t) \right]. \quad (19)$$

In the absence of backscattering $|r_j| = 0$, the functional integral Eq.(16) is Gaussian. The correlator $K_j^{(0)}(\tau) \equiv K_j(\tau)|_{r=0} = K_{j,\rho}(\tau)$ is computed at low temperature $T \ll E_C$ and at $\tau \gg E_C^{-1}$:

$$K_{j,\rho}(\tau) = \frac{\pi^2 T}{2\gamma E_{C,j}} \frac{1}{|\sin(\pi T \tau)|}. \quad (20)$$

The perturbative results (see Ref.[14]) showed that the thermoelectric properties of the system are controlled by charge and spin fluctuations at low frequencies (below $E_{C,j}$). One should notice that the effect of small but finite $|r_j|$ on the charge modes is negligible in comparison with the Coulomb blockade but it changes the low frequency dynamics of the unblocked spin modes dramatically. The correlation function can be split into charge and spin components as $K_j(\tau) = K_{j\rho}(\tau)K_{j\sigma}(\tau)$, with $K_{j\sigma}(\tau) = Z_{j\sigma}(\tau)/Z_{j\sigma}(0)$. We simply replace the $\cos[\sqrt{2}\phi_{j,\rho}(0, t)]$ in action Eq. (19) by the $\langle \cos[\sqrt{2}\phi_{j,\rho}(0, t)] \rangle_\tau = \sqrt{2\gamma E_{C,j}/\pi D} \cos[\pi N_j - \chi_{j\tau}(t)]$, with $\chi_j(t) = \pi n_{j\tau}(t) + \delta\chi_{j\tau}(t)$, $\delta\chi_{j\tau}(t) \approx \frac{\pi^2 T}{2E_{C,j}} [\cot(\pi T(t-\tau)) - \cot(\pi T t)]$ and obtain the effective action for the spin degrees of freedom in the form

$$\mathcal{S}_{\tau j} = \int dx \int_0^\beta dt \frac{v_F}{2\pi} \left[\frac{(\partial_t \phi_{j,\sigma})^2}{v_F^2} + (\partial_x \phi_{j,\sigma})^2 \right] - \int_0^\beta dt \sqrt{\frac{4D}{v_F}} \tilde{\lambda}_{j\tau}(t) \cos \left[\sqrt{2} \phi_{j,\sigma}(0, t) \right], \quad (21)$$

where

$$\tilde{\lambda}_{j\tau}(t) = \Lambda_j (-1)^{n_\tau(t)} \cos[\pi N_j - \delta\chi_{j\tau}(t)],$$

$$\Lambda_j = |r_j| \sqrt{\frac{2\gamma v_F E_{C,j}}{\pi D}}. \quad (22)$$

After performing the refermionization, our model [as shown in Eq. (21)] is mapped onto an effective Anderson model, which is described by Hamiltonian

$$H_{j,\tau}^{eff}(t) = \int \left[v_F k c_{j,k}^\dagger c_{j,k} - \tilde{\lambda}_{j\tau}(t) (c + c^\dagger) (c_{j,k} - c_{j,k}^\dagger) \right] dk, \quad (23)$$

in which the operators $c_{j,k}^\dagger$ and $c_{j,k}$ satisfying the anti-commutation relations $\{c_{j,k}, c_{j,k'}^\dagger\} = \delta(k - k')$ create and destroy chiral fermions; c is a local fermionic annihilation operator anti-commuting with $c_{j,k}^\dagger$ and $c_{j,k}$.

We see that the model is free and equivalent to a resonant level model where the leads are coupled to Majorana fermion $\eta = (c + c^\dagger)/\sqrt{2}$ on the impurity. The time dependent Hamiltonian (23) can be split into $H_{j,0}^{eff} + H'_{j,\tau}(t)$ by replacing $\tilde{\lambda}_{j\tau}(t) \rightarrow \tilde{\lambda}_{j\tau}(t)/(-1)^{n_\tau(t)}$. The time-independent Hamiltonian part $H_{j,0}^{eff}$ is $H_{j,\tau=0}^{eff}$ while the correction is

$$H'_{j,\tau}(t) = 2\Lambda_j \{ \cos[\pi N_j] - \cos[\pi N_j - \delta\chi_{j\tau}(t)] \} \eta \zeta, \quad (24)$$

with $\zeta = \int_{-\infty}^{\infty} (c_{j,k} - c_{j,k}^\dagger) dk/\sqrt{2}$ describes the Majorana fermion of the leads in the resonant level model. Our solution, being nonperturbative in $|r_j|$ and accounting for low-frequency dynamics of the spin modes, leads to the appearance of the Kondo-resonance width Γ_j in the vicinity of Coulomb peaks

$$\Gamma_j(N_j) = \frac{8\gamma E_{C,j}}{\pi^2} |r_j|^2 \cos^2(\pi N_j). \quad (25)$$

We then compute the correlation function straightforwardly and obtain the zero-order term corresponding to the Hamiltonian part $H_{j,0}^{eff}$ as

$$K_j^{(0)}\left(\frac{1}{2T} + it\right) = \frac{\pi T \Gamma_j}{\gamma E_{C,j}} \frac{1}{\cosh(\pi T t)} \times \int_{-\infty}^{\infty} \frac{e^{\omega(1/2T+it)}}{(\omega^2 + \Gamma_j^2)(1 + e^{\omega/T})} d\omega, \quad (26)$$

and the first-order term when the correction Hamiltonian part $H'_{j,\tau}(t)$ is taken into account, is

$$K_j^{(1)}\left(\frac{1}{2T} + it\right) = -\frac{4T}{E_{C,j}} \frac{|r_j|^2 \sin(2\pi N_j)}{\cosh(\pi T t)} \times \ln\left(\frac{E_{C,j}}{T + \Gamma_j}\right) \int_{-\infty}^{\infty} \frac{d\omega}{(\omega^2 + \Gamma_j^2)(1 + e^{\omega/T})} \cdot \omega e^{\omega(1/2T+it)}. \quad (27)$$

The formulas (26) and (27) will be used to calculate the thermoelectric coefficients in the next Section.

V. MAIN RESULTS

The first work of the Authors [25] considered the *weak* effects of the non-Fermi liquid behaviour in the thermoelectric transport. The approach used in [25] is based on accounting for the perturbative corrections to the transport off-diagonal coefficients and is limited by the perturbation theory domain of validity (high-temperature regime). These calculations, being very useful for understanding the flow towards the non-Fermi liquid intermediate coupling fixed point, neither become valid at the low-temperature regime, nor shed a light on reduction of the symmetry due to the emergency of the Majorana (parafermionic) states. The main idea of this work is to develop a controllable and reliable approach for the quantitative description of the Fermi-to-non-Fermi

liquid crossovers and interplay around the intermediate coupling fixed points. It therefore provides a complementary study of the model [25] and completes the theory of thermoelectrics in DCKCs.

A. Weak coupling between single- and two-channel charge Kondo circuits

In this case, for instance, we consider the left CKC is in the FL-1CK state while the right CKC is in the NFL-2CK state. We apply the correlation functions $K_1(\frac{1}{2T} + it)$ and $K_2(\frac{1}{2T} - it)$ as shown in Eqs. (15) and (26-27), respectively. The electric conductance is obtained as

$$G = \frac{\pi^2 G_C T^3}{96\gamma^3 E_{C,1}^2 E_{C,2}} F_G\left(\frac{\Gamma_2}{T}\right), \quad (28)$$

with F_G is a dimensionless parameter demonstrating the competition between the Kondo resonance of the right CKC Γ_2 and the temperature T . It is computed as

$$F_G(p_2) = \int_{-\infty}^{\infty} du J(p_2, u), \quad (29)$$

$$J(p_2, u) = \frac{[u^2 + \pi^2][u^2 + 9\pi^2]}{\cosh^2\left(\frac{u}{2}\right)[u^2 + p_2^2]}.$$

The thermoelectric coefficient is given by

$$G_T = -\frac{\pi^5 \xi G_C T^3 \Gamma_2}{72e\gamma^2 E_{C,1}^3 E_{C,2}} F_G\left(\frac{\Gamma_2}{T}\right) |r_1| \sin(2\pi N_1) - \frac{\pi G_C T^3}{360e\gamma^2 E_{C,1}^2 E_{C,2}} F_T\left(\frac{\Gamma_2}{T}\right) \left[\frac{2\pi^2 \xi \Gamma_2}{E_{C,1}} |r_1| \sin(2\pi N_1) + |r_2|^2 \ln\left(\frac{E_{C,2}}{T + \Gamma_2}\right) \sin(2\pi N_2) \right], \quad (30)$$

with

$$F_T(p_2) = \int_{-\infty}^{\infty} du u^2 J(p_2, u). \quad (31)$$

Following the discussion in Ref. [25], based on the perturbative solution, the Seebeck effect on a weak link between 1CK and 2CK is characterized by the competition between the Fermi and non-Fermi liquids (see Eq. (24) in the Ref. [25]). However, in this part, it is true for high temperature $T \gg \Gamma_2$. At very low temperature, $T \ll \Gamma_2$, the TP behaves only the FL.

1. $T \gg \Gamma_2$ limit: *Fermi-liquid on the left and non Fermi-liquid on the right CKC:*

At temperature $T \gg \Gamma_2$ the expression in Eq. (30) reproduces the perturbative result as represented in Eq. (23) of Ref.[25]. The TP is thus similar to the formula

(24) in Ref.[25]:

$$S = -\frac{4\pi^3\xi\gamma}{3e}|r_1|\frac{T}{E_{C,1}}\sin(2\pi N_1) - \frac{526\gamma}{\pi^2e}|r_2|^2\ln\left(\frac{E_{C,2}}{T}\right)\sin(2\pi N_2). \quad (32)$$

The crossover line separating the two contributions in the TP is defined as follows:

$$\frac{789}{2\pi\xi}\ln\left(\frac{E_{C,2}}{\tilde{T}}\right)\frac{E_{C,1}}{\tilde{T}} = \frac{|r_1|}{|r_2|^2}. \quad (33)$$

If $\Gamma_2 \ll T \ll \tilde{T}$, NFL-2CK behavior of the TP is predicted to be pronounced. In the opposite limit, $T \gg \tilde{T} \gg \Gamma_2$, the FL-1CK regime with the weak NFL-2CK corrections is expected.

2. $T \ll \Gamma_2$ limit: fully Fermi-liquid regime:

At temperature $T \ll \Gamma_2$ the expression in Eq. (30) induces the linear temperature term in the square brackets. The TP thus behaves the FL characteristic as

$$S = -\frac{7682\pi^3\xi\gamma}{5523e}\left[|r_1|\frac{T}{E_{C,1}}\sin(2\pi N_1) + \frac{1431}{3841\pi^2\xi}|r_2|^2\ln\left(\frac{E_{C,2}}{\Gamma_2}\right)\frac{T}{E_{C,2}}\sin(2\pi N_2)\right]. \quad (34)$$

In summary, in the situation of the weak coupling between single- and two-channel charge Kondo circuits, there exist two energy scales Γ_2 ($\Gamma_2 \leq (8\gamma/\pi^2)E_{C,2}|r_2|^2$) and \tilde{T} of temperature in the regime (0, $E_{C,2}$) in which one finds more chances for the FL picture than the NFL one.

B. Weak coupling between two two-channel charge Kondo circuits

We take into account both $K_j^{(0)}(\frac{1}{2T} + it)$, we have

$$G = \frac{G_C T^2}{24\gamma^2 E_{C,1} E_{C,2}} F_C\left(\frac{\Gamma_1}{T}, \frac{\Gamma_2}{T}\right), \quad (35)$$

with

$$F_C(p_1, p_2) = \int_{-\infty}^{\infty} dz \int_{-\infty}^{\infty} du F(p_1, p_2, z, u), \quad (36)$$

$$F(p_1, p_2, z, u) = \frac{p_1 p_2 u [u^2 + 4\pi^2]}{\sinh\left(\frac{u}{2}\right) [\cosh(z) + \cosh\left(\frac{u}{2}\right)]} \times \frac{1}{\left[\left(z + \frac{u}{2}\right)^2 + p_1^2\right] \left[\left(z - \frac{u}{2}\right)^2 + p_2^2\right]}. \quad (37)$$

The integral in Eq. (10) gives the zero value when we apply $K_{1,2}^{(0)}(\frac{1}{2T} \pm it)$ for both sides: $G_T^{(0)} =$

0. We therefore need to consider the first order of the correlation function. We take into account, for instance, $K_1^{(0)}(\frac{1}{2T} + it) K_2^{(1)}(\frac{1}{2T} - it)$ and $K_1^{(1)}(\frac{1}{2T} + it) K_2^{(0)}(\frac{1}{2T} - it)$, we obtain the lowest order (we consider the model in the vicinity of the intermediate coupling fixed point) non-zero contribution to thermoelectric coefficient as follows

$$G_T^{(1)} = -\frac{G_C T^3}{24e\gamma\pi E_{C,1} E_{C,2}} \times \left\{ \frac{|r_1|^2}{\Gamma_1} \ln\left(\frac{E_{C,1}}{T + \Gamma_1}\right) \sin(2\pi N_1) F_{T,s}\left(\frac{\Gamma_1}{T}, \frac{\Gamma_2}{T}\right) + \frac{|r_2|^2}{\Gamma_2} \ln\left(\frac{E_{C,2}}{T + \Gamma_2}\right) \sin(2\pi N_2) F_{T,m}\left(\frac{\Gamma_1}{T}, \frac{\Gamma_2}{T}\right) \right\}, \quad (38)$$

where

$$F_{T,s}(p_1, p_2) = \int_{-\infty}^{\infty} dz \int_{-\infty}^{\infty} du \left(z + \frac{u}{2}\right) z F(p_1, p_2, z, u), \quad (39)$$

$$F_{T,m}(p_1, p_2) = \int_{-\infty}^{\infty} dz \int_{-\infty}^{\infty} du \left(z - \frac{u}{2}\right) z F(p_1, p_2, z, u). \quad (40)$$

The Eqs. (35-38) are the central results of this part. By varying parameters such as temperature, gate voltages, and/or reflection amplitudes at the QPCs, one can achieve four different regimes of the thermoelectric transport. The details of the calculations for the electric conductance and the thermal coefficient are represented in the Appendix. We show the formulas for the TP in each regime in four segments below.

1. $T \gg (\Gamma_1, \Gamma_2)$, fully non-Fermi-liquid regime:

The TP demonstrates the weak NFL behavior at ‘‘high’’ temperature: $T \gg (\Gamma_1, \Gamma_2)$ as

$$S = -\frac{3\pi^2\gamma}{16e}\left[|r_1|^2\ln\left(\frac{E_{C,1}}{T}\right)\sin(2\pi N_1) + |r_2|^2\ln\left(\frac{E_{C,2}}{T}\right)\sin(2\pi N_2)\right]. \quad (41)$$

The similarity between Eq. (41) and Eq. (28) of Ref. [25] implies that the regime $T \gg (\Gamma_1, \Gamma_2)$ reproduces the perturbative result. The Kondo-resonance Γ_j is equal to zero at the Coulomb peaks and increased when the gate voltage N_j goes out of the half integer values. This situation occurs at the centre of the (N_1, N_2) window (if one considers $0 \leq N_1, N_2 \leq 1$). Due to the logarithmic dependent on temperature but small value of TP [see Eq. (41)] it is so-called a weak non-Fermi-liquid picture. The maximum value of TP $S_{max} \sim |r_1|^2 \ln\left(\frac{E_{C,1}}{T}\right) + |r_2|^2 \ln\left(\frac{E_{C,2}}{T}\right)$ is reached when $N_1 = N_2 = 0.25$.

2. $\Gamma_1 \ll T \ll \Gamma_2$, *weak non-Fermi-liquid on the left and Fermi-liquid on the right CKC:*

Let us recall that the Kondo resonances' widths Γ_1, Γ_2 depend on the gate voltages and therefore compete with temperature effects in the vicinity of the Coulomb peaks. With a given temperature this situation occurs when the QD 1 is closer to a Coulomb peak (N_1 is closer to a half integer value) than the QD 2 is. The TP includes two components: weak non-Fermi-liquid and Fermi-liquid characteristics as

$$S = -\frac{256\gamma}{75e\pi^2} \left[|r_1|^2 \ln \left(\frac{E_{C,1}}{T} \right) \sin(2\pi N_1) + \frac{25\pi^3}{128} \frac{T}{\Gamma_2} |r_2|^2 \ln \left(\frac{E_{C,2}}{\Gamma_2} \right) \sin(2\pi N_2) \right]. \quad (42)$$

The crossover line between two regimes is defined as

$$\frac{E_{C,2}}{T^*} \ln \left(\frac{E_{C,1}}{T^*} \right) = \frac{25\pi^5}{1024\gamma \cos^2(\pi N_2)} \frac{1}{|r_1|^2} \times \ln \left(\frac{\pi^2}{8\gamma |r_2|^2 \cos^2(\pi N_2)} \right) \quad (43)$$

The NFL behavior is dominated if $T \ll T^*$ while the FL property is predicted at the opposite limit $T \gg T^*$.

3. $\Gamma_2 \ll T \ll \Gamma_1$, *Fermi-liquid on the left and weak non-Fermi-liquid on the right CKC:*

This situation is opposite to the case discussed in the Section VB2. The regime is achieved when the QD 2 is closer to a Coulomb blockade peak than the QD 1 is. The TP is characterized by the FL on the left and weak NFL effect on the right CKC as

$$S = -\frac{256\gamma}{75e\pi^2} \left[\frac{25\pi^3}{128} \frac{T}{\Gamma_1} |r_1|^2 \ln \left(\frac{E_{C,1}}{\Gamma_1} \right) \sin(2\pi N_1) + |r_2|^2 \ln \left(\frac{E_{C,2}}{T} \right) \sin(2\pi N_2) \right]. \quad (44)$$

The crossover line between two regimes is defined as

$$\frac{E_{C,1}}{T^{**}} \ln \left(\frac{E_{C,2}}{T^{**}} \right) = \frac{25\pi^5}{1024\gamma \cos^2(\pi N_1)} \frac{1}{|r_2|^2} \times \ln \left(\frac{\pi^2}{8\gamma |r_1|^2 \cos^2(\pi N_1)} \right) \quad (45)$$

The NFL behavior is dominated if $T \ll T^{**}$ while the FL property is predicted at the opposite limit $T \gg T^{**}$. If the two CKCs are symmetry, $T^{**} = T^*$.

4. $T \ll (\Gamma_1, \Gamma_2)$, *fully Fermi-liquid regime:*

When the temperature is decreased to approach the zero value, the TP of the system behaves in accordance

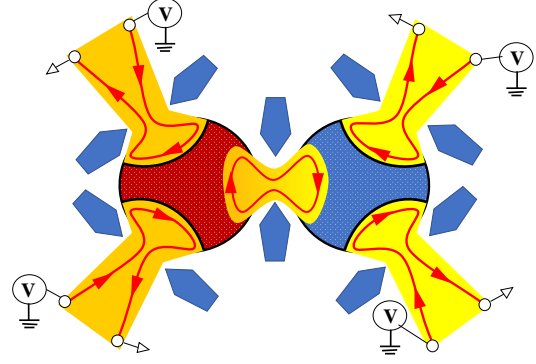


FIG. 2. Schematic of a strong coupling between two charge Kondo circuits. Notations are the same as on Figure 1 with two distinct differences: i) different color scheme used for the left (orange, hot) and right (yellow, cold) parts of the circuit; ii) the central part of the system is modified. The tunnel contact in the center of Fig 1 is replaced by almost transparent QPC. The chiral edge mode strongly couples QD1 and QD2. The temperature gradient (shown by continuous change of colour from orange to yellow) is applied across the central QPC.

with the nonperturbative FL picture:

$$S = -\frac{3\pi\gamma T}{7e} \left[\frac{|r_1|^2}{\Gamma_1} \ln \left(\frac{E_{C,1}}{\Gamma_1} \right) \sin(2\pi N_1) + \frac{|r_2|^2}{\Gamma_2} \ln \left(\frac{E_{C,2}}{\Gamma_2} \right) \sin(2\pi N_2) \right]. \quad (46)$$

The TP is a linear function of the temperature. However, the pre-factors are giant when both QDs are in the vicinities of the Coulomb peaks. The system has strong FL property.

C. Discussion

The investigation of TP for the weak coupling between two CKCs in both cases: 1CK - 2CK and 2CK - 2CK shows the competition between the FL and NFL picture. However, the windows of parameters to observe the FL property are much broader than the windows to access the NFL one. The reason is that the NFL intermediate coupling fixed points of MCK are hyperbolic and therefore unstable. The results of this work not only cover the perturbative accessible regimes, which have been represented in Ref. [25], but also show a rich property of the TP in different domains of parameters.

Extending the proposal of the weak coupling between two CKCs [25] to the regime of almost transparent QPC in the central area of the DCKC, the very recent experiment [53] and theory [54, 55] have investigated the strong coupling limit. Let us comment on the connection between the weak and strong coupling regimes of the DCKCs. In Ref. [25] we have considered the DCKC weakly connecting 1CK-1CK or 1CK-2CK or 2CK-2CK. The same realization for the strong coupling of two

Kondo simulators has also been theoretically suggested in [25] and experimentally realized recently in [53] for 1CK-1CK coupling [59]. One of the most exciting theoretical predictions of the two-impurity single channel Kondo effect [61–63] is a possibility to map the model under certain assumptions onto the 2CK Hamiltonian. Interestingly, the Refs. [53–55] showed that at the triple degeneracy point of the DCKC Z_3 symmetry and corresponding local parafermion emerge. It is straightforward to extend the idea [25] to MCK-NCK strong coupling (see Fig 2). Suppose that there are $M > 1$ identical QPCs in the left hand side of the DCKC and $N > 1$ identical QPCs in the right side of it. The total degeneracy is $M + 1 + N$ and corresponding emergent local symmetry is Z_{M+N+1} . There are three important (M, N) realizations accessible through existing experimental setups: i) (2, 1) or (1, 2) connecting 1CK and 2CK with emergent symmetry Z_4 ; ii) (2, 2) and iii) (3, 1) or (1, 3) with emergent symmetry Z_5 . Corresponding weak link setups are characterized by the symmetries: i) $U(1) \times Z_2$; ii) $Z_2 \times Z_2$ and iii) $U(1) \times Z_3$. As the weak coupling regimes of ii) and iii) are clearly distinct, being characterized by both different symmetries and different Lorenz ratios (see Ref. [29] for more details), it is interesting to examine regimes ii) and iii) in the strong coupling limit. In particular it is important to understand the symmetry of *local* parafermion emerging in the strong link setup. In addition, switching between different intermediate coupling fixed points results in crossovers between various fractionalized modes manifesting itself in distinctly different regimes of the charge and heat transport.

The weak link regime discussed in this manuscript was analysed using a standard approach based on the transport integrals [25]. The validity of this approach is justified by an assumption that both temperature and voltage drops occur exactly at the central tunnel barrier. As a result, both the left and the right parts of the DCKC are considered at thermal and mechanical equilibrium being characterized by certain temperature T and chemical potential μ . This approach is clearly invalid for the strong link between two sides of the Kondo simulator where both the temperature and the voltage changes continuously across the central QPC. The full-fledged linear response theory of the charge and heat transport across the strong link of the two-site Kondo simulators can be constructed by using *Luttinger's pseudo-gravitational approach* [64, 65] or *thermo-mechanical potential* [66, 67] method in combination with Kubo equations. The theory beyond linear response requires also using Keldysh formalism [66, 67] and represents an interesting and important direction for the future investigation.

VI. CONCLUSION

In this work, we revisited the thermoelectric transport at the weak link of the DCKC model proposed in

the Ref. [25]. The Abelian bosonization approach is used for both 1CK and 2CK setup while the refermionization technique is applied in order to solve the 2CK model nonperturbatively. We show the different windows of the parameter set where the TP behaves either the full FL or NFL characteristics or the competition between these properties. The nonperturbative results not only cover the perturbative results but also be applicable in the lower temperature regime $T < |r_j|^2 E_{C,j}$. We predict that the TP is enhanced in the DCKC in comparison with the single CKC setup. Indeed, a complex charge Kondo circuit which shows the diversity of the competition between the FL and NFL properties, can be a potential thermoelectric material. Moreover, we propose to use the experimental implementation in Ref. [53] for investigating the different parafermion contributions to the quantum thermoelectricity when the coupling between QDs is switched from weak to strong.

ACKNOWLEDGEMENT

This research in Hanoi is funded by Vietnam Academy of Science and Technology (program for Physics development) under grant number KHCBVL.06/23-24. The work of M.N.K is conducted within the framework of the Trieste Institute for Theoretical Quantum Technologies (TQT). M.N.K also acknowledges the support from the Alexander von Humboldt Foundation for the research visit to IFW Dresden.

APPENDIX

In this Appendix we represent the details of the different approaches at different limits in order to obtain the results shown in the Subsection V B.

1, If $p_1 \rightarrow 0, p_2 \rightarrow 0$, we have:

$$\lim_{p_1 \rightarrow 0} \frac{p_1}{\left(z + \frac{u}{2}\right)^2 + p_1^2} = \pi \delta\left(z + \frac{u}{2}\right), \quad (47)$$

$$\lim_{p_2 \rightarrow 0} \frac{p_2}{\left(z - \frac{u}{2}\right)^2 + p_2^2} = \pi \delta\left(z - \frac{u}{2}\right). \quad (48)$$

As a result

$$\begin{aligned} & \lim_{p_2 \rightarrow 0} \frac{F_{T,m}(p_1 \rightarrow 0, p_2)}{p_2} \\ &= \lim_{p_2 \rightarrow 0} \int_{-\infty}^{\infty} du \frac{\pi u^3 [u^2 + 4\pi^2]}{\sinh[u] [u^2 + p_2^2]} \\ &= \int_{-\infty}^{\infty} du \frac{\pi u [u^2 + 4\pi^2]}{\sinh[u]} = \frac{3\pi^5}{4}, \end{aligned} \quad (49)$$

and, finally

$$\lim_{p_1 \rightarrow 0} \frac{F_{T,s}(p_1, p_2 \rightarrow 0)}{p_1} = \frac{3\pi^5}{4}. \quad (50)$$

We obtain the electric conductance as

$$G^{(0)} = \frac{\pi^2 G_C T^2}{6\gamma^2 E_{C,1} E_{C,2}}, \quad (51)$$

and the thermoelectric coefficient as

$$G_T^{(1)} = -\frac{\pi^4 G_C T^2}{32e\gamma E_{C,1} E_{C,2}} \left[|r_1|^2 \ln \left(\frac{E_{C,1}}{T} \right) \sin(2\pi N_1) + |r_2|^2 \ln \left(\frac{E_{C,2}}{T} \right) \sin(2\pi N_2) \right]. \quad (52)$$

2, If $p_1 \rightarrow 0, p_2 \gg 1$ we have:

$$F_C(p_1 \rightarrow 0, p_2) = \int_{-\infty}^{\infty} du \frac{\pi p_2 u [u^2 + 4\pi^2]}{\sinh[u] [u^2 + p_2^2]},$$

$$F_C(p_1 \rightarrow 0, p_2 \gg 1) = \frac{\pi}{p_2} \int_{-\infty}^{\infty} du \frac{u [u^2 + 4\pi^2]}{\sinh[u]} = \frac{9\pi^5}{4p_2} \quad (53)$$

and

$$F_{T,m}(p_1 \rightarrow 0, p_2 \gg 1) = \frac{\pi}{p_2} \int_{-\infty}^{\infty} du \frac{u^3 [u^2 + 4\pi^2]}{\sinh[u]} = \frac{3\pi^7}{2p_2}. \quad (54)$$

The calculation of the $F_{T,s}$ is a bit complicated, which concerns the principal value (PV) as follows.

$$\begin{aligned} \frac{F_{T,s}(p_1 \rightarrow 0, p_2 \gg 1)}{p_1} &= \frac{1}{p_2} \text{PV} \int_{-\infty}^{\infty} dz \int_{-\infty}^{\infty} du \\ &\times \frac{uz [u^2 + 4\pi^2]}{\left(z + \frac{u}{2}\right) \sinh\left(\frac{u}{2}\right) [\cosh(z) + \cosh\left(\frac{u}{2}\right)]} \\ &= \frac{8}{p_2} \int_{-\infty}^{\infty} dp \int_{-\infty}^{\infty} dq \left\{ \frac{q [q^2 + 4\pi^2]}{\sinh(q) \cosh(p/2) \cosh(p/2 - q)} \right. \\ &\left. - \frac{\tanh(p/2) q^2 [q^2 + 4\pi^2]}{p \cosh(p/2 + q) \cosh(p/2 - q)} \right\} = \frac{192\pi^4}{25p_2}. \quad (55) \end{aligned}$$

The electric conductance G and the thermoelectric coefficient G_T is computed at the first non-zero term in the nonperturbative treatment are

$$G^{(0)} = \frac{3G_C \pi^5 T^3}{32\gamma^2 \Gamma_2 E_{C,1} E_{C,2}}, \quad (56)$$

$$G_T^{(1)} = -\frac{8G_C \pi^3 T^3}{25e\gamma E_{C,1} E_{C,2} \Gamma_2} \left[|r_1|^2 \ln \left(\frac{E_{C,1}}{T} \right) \sin(2\pi N_1) + \frac{25\pi^3 T}{128 \Gamma_2} |r_2|^2 \ln \left(\frac{E_{C,2}}{\Gamma_2} \right) \sin(2\pi N_2) \right]. \quad (57)$$

3, $p_1 \gg 1, p_2 \rightarrow 0$: This limit is opposite to the second limit. The calculation process is the same as the above one.

$$F_C(p_1 \gg 1, p_2 \rightarrow 0) = \frac{\pi}{p_1} \int_{-\infty}^{\infty} du \frac{u [u^2 + 4\pi^2]}{\sinh[u]} = \frac{9\pi^5}{4p_1}, \quad (58)$$

$$F_{T,m}(p_1 \gg 1, p_2 \rightarrow 0) = \frac{1}{p_2} \text{PV} \int_{-\infty}^{\infty} dz \int_{-\infty}^{\infty} du$$

$$\times \frac{uz [u^2 + 4\pi^2]}{\left(z - \frac{u}{2}\right) \sinh\left(\frac{u}{2}\right) [\cosh(z) + \cosh\left(\frac{u}{2}\right)]} = \frac{192\pi^4}{25p_1}, \quad (59)$$

$$F_{T,s}(p_1 \gg 1, p_2 \rightarrow 0) = \frac{3\pi^7}{2p_1}. \quad (60)$$

The electric conductance is

$$G^{(0)} = \frac{3G_C \pi^5 T^3}{32\gamma^2 E_{C,1} E_{C,2} \Gamma_1}, \quad (61)$$

and the thermoelectric coefficient is

$$G_T^{(1)} = -\frac{8G_C \pi^3 T^3}{25e\gamma E_{C,1} E_{C,2} \Gamma_1}$$

$$\times \left\{ \frac{25\pi^3 T}{128 \Gamma_1} |r_1|^2 \ln \left(\frac{E_{C,1}}{\Gamma_1} \right) \sin(2\pi N_1) + |r_2|^2 \ln \left(\frac{E_{C,2}}{T} \right) \sin(2\pi N_2) \right\}. \quad (62)$$

4, If $p_1 \gg 1, p_2 \gg 1$, we simply remove the terms which are summed with p_1^2 and p_2^2 in the denominator of the formula (37). We then obtain:

$$F_C(p_1 \gg 1, p_2 \gg 1) = \frac{1}{p_1 p_2} \int_{-\infty}^{\infty} dz \int_{-\infty}^{\infty} du$$

$$\times \frac{u [u^2 + 4\pi^2]}{\sinh\left[\frac{u}{2}\right] [\cosh(z) + \cosh\left(\frac{u}{2}\right)]} = \frac{64\pi^4}{5p_1 p_2}. \quad (63)$$

$$F_{T,m}(p_1 \gg 1, p_2 \gg 1) = \frac{1}{p_1 p_2} \int_{-\infty}^{\infty} dz \int_{-\infty}^{\infty} du$$

$$\times \frac{\left(z - \frac{u}{2}\right) uz [u^2 + 4\pi^2]}{\sinh\left[\frac{u}{2}\right] [\cosh(z) + \cosh\left(\frac{u}{2}\right)]} = \frac{192\pi^6}{35p_1 p_2}. \quad (64)$$

$$F_{T,s}(p_1 \gg 1, p_2 \gg 1) = \frac{1}{p_1 p_2} \int_{-\infty}^{\infty} dz \int_{-\infty}^{\infty} du$$

$$\times \frac{\left(z + \frac{u}{2}\right) uz [u^2 + 4\pi^2]}{\sinh\left[\frac{u}{2}\right] [\cosh(z) + \cosh\left(\frac{u}{2}\right)]} = \frac{192\pi^6}{35p_1 p_2}. \quad (65)$$

The electric conductance and the thermoelectric coefficient in this limit are

$$G = \frac{8G_C \pi^4 T^4}{15\gamma^2 E_{C,1} E_{C,2} \Gamma_1 \Gamma_2}, \quad (66)$$

$$G_T^{(1)} = -\frac{24G_C \pi^5 T^5}{105e\gamma E_{C,1} E_{C,2} \Gamma_1 \Gamma_2}$$

$$\times \left\{ \frac{|r_1|^2}{\Gamma_1} \ln \left(\frac{E_{C,1}}{T + \Gamma_1} \right) \sin(2\pi N_1) + \frac{|r_2|^2}{\Gamma_2} \ln \left(\frac{E_{C,2}}{T + \Gamma_2} \right) \sin(2\pi N_2) \right\}. \quad (67)$$

-
- [1] G. Snyder and E. Toberer, Nat. Mater. **7**, 105 (2008).
- [2] T. J. Seebeck, Abh. Akad. Wiss. Berlin **1820-21**, 289 (1822).
- [3] J. F. Li, W.S. Liu, L.D. Zhao, and M. Zhou, NPG Asia Mater. **2**, 152 (2010).
- [4] Y. Du, K. F. Cai, S. Chen, H. Wang, S. Z. Shen, R. Donelson, and T. Lin, Sci. Rep. **5**, 6144 (2015).
- [5] M. S. Dresselhaus, G. Chen, M. Y. Tang, R. G. Yang, H. Lee, D. Z. Wang, Z. F. Ren, J. P. Fleurial, P. Gogna, Adv. Mater. **19**, 1043 (2007).
- [6] G. Chen, M. S. Dresselhaus, G. Dresselhaus, J. P. Fleurial, and T. Caillat, Int. Mater. Rev. **48**, 45 (2003).
- [7] Y. M. Blanter and Y. V. Nazarov, *Quantum Transport: Introduction to Nanoscience* (Cambridge University Press, Cambridge, 2009).
- [8] K. Kikoin, M. N. Kiselev, and Y. Avishai, *Dynamical Symmetry for Nanostructures. Implicit Symmetry in Single-Electron Transport Through Real and Artificial Molecules* (Springer, New York, 2012).
- [9] A. A. M. Staring, L. W. Molenkamp, B. W. Alphenhaar, H. van Houten, O. J. A. Buyk, M. A. A. Mablesone, C. W. J. Beenakker, and C. T. Foxon, Europhys. Lett. **22**, 57 (1993).
- [10] M. Turek and K. A. Matveev, Phys. Rev. B **65**, 115332 (2002).
- [11] K. Flensberg, Phys. Rev. B **48**, 11156 (1993).
- [12] K. A. Matveev, Phys. Rev. B **51**, 1743 (1995).
- [13] A. Furusaki and K. A. Matveev, Phys. Rev. Lett. **75**, 709 (1995).
- [14] A. V. Andreev and K. A. Matveev, Phys. Rev. Lett. **86**, 280 (2001); Phys. Rev. B **66**, 045301 (2002).
- [15] K. Le Hur, Phys. Rev. B **64**, 161302(R) (2001).
- [16] K. Le Hur and G. Seelig, Phys. Rev. B **65**, 165338 (2002).
- [17] J. Kondo, Prog. Theor. Phys. **32**, 37 (1964).
- [18] A. Hewson, *The Kondo Problem to Heavy Fermions* (Cambridge University Press, Cambridge, England, 1993).
- [19] A. M. Tsvelik and P. B. Wiegmann, Adv. in Phys., **32**, 453 (1983).
- [20] N. Andrei, K. Furuya, and J. H. Lowenstein, Rev. Mod. Phys. **55**, 331 (1983).
- [21] L. Kouwenhoven and L. I. Glazman, Phys. World **14**, 33 (2001).
- [22] R. Scheibner, H. Buhmann, D. Reuter, M. N. Kiselev, and L. W. Molenkamp, Phys. Rev. Lett. **95**, 176602 (2005).
- [23] T. K. T. Nguyen, M. N. Kiselev, and V. E. Kravtsov, Phys. Rev. B **82**, 113306 (2010).
- [24] T. K. T. Nguyen and M. N. Kiselev, Phys. Rev. B **92**, 045125 (2015).
- [25] T. K. T. Nguyen, M. N. Kiselev, Phys. Rev. B **97**, 085403 (2018).
- [26] A. V. Parafilo, T. K. T. Nguyen, and M. N. Kiselev, Phys. Rev. B **105**, L121405 (2022).
- [27] T. K. T. Nguyen and M. N. Kiselev, Commun. Phys. **32**, 331 (2022).
- [28] A. V. Parafilo and T. K. T. Nguyen, Commun. Phys. **33**, 1 (2023).
- [29] M. N. Kiselev, arXiv: 2304.10872 (2023).
- [30] E. Sela, A. K. Mitchell, and L. Fritz, Phys. Rev. Lett. **106**, 147202 (2011).
- [31] A. K. Mitchell, L. A. Landau, L. Fritz, and E. Sela, Phys. Rev. Lett. **116**, 157202 (2016).
- [32] L. A. Landau, E. Cornfeld, and E. Sela, Phys. Rev. Lett. **120**, 186801 (2018).
- [33] G. A. R. van Dalum, A. K. Mitchell, and L. Fritz, Phys. Rev. B **102**, 041111(R) (2020).
- [34] T. K. T. Nguyen and M. N. Kiselev, Commun. Phys. **30**, 1 (2020).
- [35] T. K. T. Nguyen, A. V. Parafilo, H. Q. Nguyen, and M. N. Kiselev, Phys. Rev. B **107**, L201402 (2023).
- [36] Z. Iftikhar, S. Jezouin, A. Anthore, U. Gennser, F. D. Parmentier, A. Cavanna and F. Pierre, Nature **526**, 233 (2015).
- [37] Z. Iftikhar, A. Anthore, A. K. Mitchell, F. D. Parmentier, U. Gennser, A. Ouerghi, A. Cavanna, C. Mora, P. Simon, and F. Pierre, Science **360**, 1315 (2018).
- [38] Ph. Nozières and A. Blandin, J. Phys. **41**, 193 (1980).
- [39] D. Cox and A. Zawadowski, Advances in Physics **47**, 599 (1998).
- [40] I. Affleck and A. W. W. Ludwig, Phys. Rev. B **48**, 7297 (1993).
- [41] N. Andrei and C. Destri, Phys. Rev. Lett. **52**, 364 (1984).
- [42] M. Fabrizio, A. O. Gogolin, and P. Nozières, Phys. Rev. Lett. **74**, 4503 (1995).
- [43] M. Fabrizio, A. O. Gogolin, and P. Nozières, Phys. Rev. B **51**, 16088 (1995).
- [44] A. O. Gogolin, A. A. Nersesyan, and A. M. Tsvelik, *Bosonization Approach to Strongly Correlated Systems* (Cambridge University Press, Cambridge, England, 1998).
- [45] V. J. Emery and S. Kivelson, Phys. Rev. B **46**, 10812 (1992).
- [46] A. B. Zamolodchikov and V. A. Fateev, ZhETF **89**, 380 (1985) [Sov. Phys. JETP **62**, 215 (1985)].
- [47] H. Yi and C. L. Kane, Phys. Rev. B **57**, R5579 (1998).
- [48] H. Yi, Phys. Rev. B **65**, 195101 (2002).
- [49] I. Affleck, M. Oshikawa, and H. Saleur, Nucl. Phys. B **594**, 535 (2001).
- [50] C. Nayak, S. H. Simon, A. Stern, M. Freedman, and S. D. Sarma, Rev. Mod. Phys. **80**, 1083 (2008).
- [51] J. Alicea and P. Fendley, Annu. Rev. Condens. Matter Phys. **7**, 119 (2016).
- [52] T. K. T. Nguyen and M. N. Kiselev, Phys. Rev. Lett. **125**, 026801 (2020).
- [53] W. Pouse, L. Peeters, C. L. Hsueh, U. Gennser, A. Cavanna, M. A. Kastner, A. K. Mitchell, and D. Goldhaber-Gordon, Nat. Phys. (2023).
- [54] D. B. Karki, E. Boulat, and C. Mora, Phys. Rev. B **105**, 245418 (2022).
- [55] D. B. Karki, E. Boulat, W. Pouse, D. Goldhaber-Gordon, A. K. Mitchell, and C. Mora, Phys. Rev. Lett. **130**, 146201 (2023).
- [56] I. L. Aleiner and L. I. Glazman, Phys. Rev. B **57**, 9608 (1998).
- [57] T. Giamarchi, *Quantum Physics in One Dimension* (Oxford University Press, Oxford, UK, 2003).
- [58] There is a missing factor 2π in Eq. (13) of Ref. [25], which consequently requires to put an additional prefactor 2π in all formulas of thermoelectric coefficient G_T and thermopower S thereafter.
- [59] Historically, the idea of Double-Large-Dot Charge

Kondo configuration has been first theoretically proposed in [60] for the *thermodynamic* investigation of the fractional $e/2$ charge Coulomb Blockade capacitance peaks.

- [60] K. Le Hur, Phys. Rev. B **67**, 125311 (2003).
- [61] B. A. Jones and C. M. Varma, Phys. Rev. Lett. **58**, 843 (1987); B. A. Jones, C. M. Varma, and J. W. Wilkins, *ibid.* **61**, 125 (1988).
- [62] J. Gan, Phys. Rev. Lett. **74**, 2583 (1995); Phys. Rev. B **51**, 8287 (1995).
- [63] A. K. Mitchell, E. Sela, and D. E. Logan, Phys. Rev. Lett. **108**, 086405 (2012).
- [64] J. M. Luttinger, Phys. Rev. **135**, A1505 (1964).
- [65] B. S. Shastry, Rep. Prog. Phys. **72**, 016501 (2009).
- [66] F. G. Eich, M. Di Ventra, and G. Vignale Phys. Rev. Lett. **112**, 196401 (2014).
- [67] F. G. Eich, A. Principi, M. Di Ventra, and G. Vignale Phys. Rev. B **90**, 115116 (2014).